Delft University of Technology

Masters in Systems and Control

Robust Control Assignment

Part 3

January 15, 2021

Contents

List of Figures

1 Motivation, overview

In this part of the assignment robust control aspects are also considered. First the previously designed H_∞ controller is analysed to also test robust stability and performance. It is shown that some tools used for robustness analysis can also be used to test nominal performance. In the second part new controller is designed which satisfies also the robustness requirements.

It is given that the plant has input and output uncertainty in its extended model. In Section 2.4 the possible derivation of the uncertainty weights is described. Section 2.6 contains all the analysis performed to check nominal stability, nominal performance, robust stability and robust performance. Section 2.7 describes the relationship between the μ value output of the nominal performance analysis and the objective function used for H_∞ controller synthesis.

In the second part (Section 3) a robust controller is designed using the D-K iteration method manually and via the automated MATLAB *dksyn* function (Robust Control Toolbox). The ω frequency points that are used for the D scaling matrix construction in the iteration is specified manually and these are the same points that were used for the analysis previously. Also the designed robust controller is compared to the nominal controller using time-domain closed loop simulations and relevant frequency domain plots (Section 3.3).

2 Robustness analysis

This section covers several aspects regarding the system behaviour under uncertainty. More specifically, the uncertainty between the inputs β and τ_e and the outputs ω and z is characterized by means of two weights (W_i, W_o) and two perturbation matrices (Δ_i, Δ_o), added to the nominal system as input and output multiplicative uncertainty, respectively.

In this way, an uncertainty block can be defined in the following way:

$$\Delta = \begin{bmatrix} \delta_{i1} & 0 & 0 & 0 \\ 0 & \delta_{i2} & 0 & 0 \\ 0 & 0 & \delta_{o1} & 0 \\ 0 & 0 & 0 & \delta_{o2} \end{bmatrix} \tag{1}$$

This can be easily implemented in Matlab using the Robust Toolbox notation:

$$blk = [1\ 1; 1\ 1; 1\ 1; 1\ 1] \tag{2}$$

In which it is specified that the delta values can be complex, are top-bounded by 1, and the uncertainty matrix have structure (have different values in the diagonal and zeros everywhere else).

2.1 Block diagram of the system

Figure 1 shows the negative feedback block diagram for the model of the controlled floating wind turbine. For this part, the design will be performed for a model without the wind disturbance input. This implies that the plant $G(s)$ is the transfer function that relates inputs β and τ_e and the outputs ω and z.

In the block diagram one can observe the weights for the error and controller outputs (W_p,W_u), the model plant G, and the controller K. In addition to this, there have been included the uncertainty weights (W_i, W_o) and their corresponding perturbation matrices (Δ_i, Δ_o).

The most relevant signals in the design are the reference input (w), the controller signal output (u), the output error (v), the weighted uncertainty signals $(y_{\Delta i}, y_{\Delta o})$ and the input and output multiplicative uncertainties $(u_{\Delta i}, u_{\Delta o})$. Finally, the outputs (z_1) and (z_2) show the weighted system's error and controller's output, respectively.

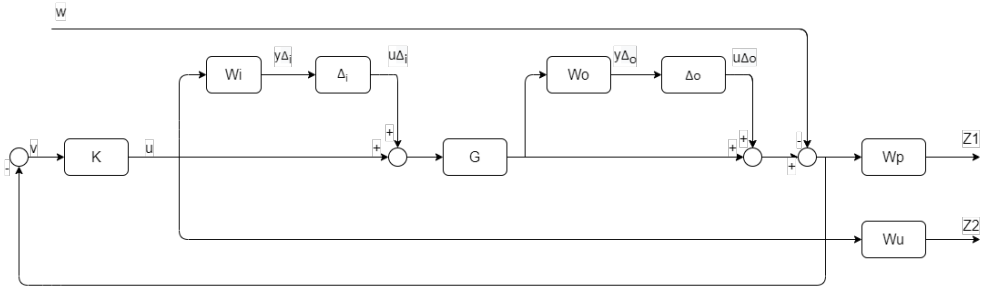

Figure 1: Block diagram of the uncertain model with negative feedback

The uncertainty weights have the following structure, in which one can observe that the diagonal terms are the same:

$$W_i = \begin{bmatrix} W_{i_1} & 0 \\ 0 & W_{i_2} \end{bmatrix} \tag{3}$$

$$W_o = \begin{bmatrix} W_{o_1} & 0 \\ 0 & W_{o_2} \end{bmatrix} \tag{4}$$

As a reminder, the performance weights are hereafter showed:

$$W_{i_1} = W_{i_2} = \frac{\frac{1}{16\pi}s + 0.3}{\frac{1}{64\pi}s + 1} \tag{5}$$

$$W_{o_1} = W_{o_2} = \frac{0.05s + 0.2}{0.01s + 1} \tag{6}$$

$$W_p = \begin{bmatrix} W_{p11} & 0 \\ 0 & 0.2 \end{bmatrix} \tag{7}$$

$$W_u = \begin{bmatrix} 0.01 & 0 \\ 0 & Wu_{22} \end{bmatrix} \tag{8}$$

$$W_{p11} = \frac{s + 4.524}{1.8s + 4.524 \cdot 10^{-4}} \tag{9}$$

$$W_{u22} = \frac{5 \cdot 10^{-3}s^2 + 7 \cdot 10^{-4}s + 5 \cdot 10^{-5}}{s^2 + 14 \cdot 10^{-4}s + 10^{-6}} \tag{10}$$

2.2 Mathematical description of the diagram

The generalized plant can be obtained by including the blocks inside the green area in Figure 2 into a common block P.

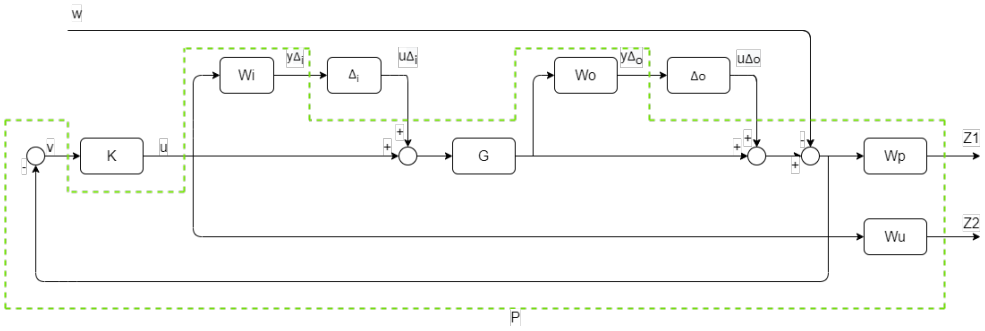

Figure 2: Block diagram of the uncertain model with negative feedback

The output $Z1$ is composed of the multiplication of the weight W_p and the system error, this is, the subtraction of the reference input w and the signal u multiplied by the modified plant. Moreover, the output $Z2$ is directly the input from the controller (u) multiplied by W_u, while the output signal v is the previously mentioned system error.

In addition to this, the weighted input uncertainty signal $y_{\Delta i}$ is composed by the multiplication of the controller input u and the weight W_i, while the weighted output uncertainty signal $y_{\Delta o}$ is the output of the plant G multiplied by the weight W_o.

Taking into account these relationships, the generalized plant P can be obtained:

$$\begin{bmatrix} y_{\Delta i} \\ y_{\Delta o} \\ z_1 \\ z_2 \\ v \end{bmatrix} = \underbrace{\begin{bmatrix} 0 & 0 & 0 & W_i \\ W_oG & 0 & 0 & W_oG \\ W_pG & W_p & -W_p & W_pG \\ 0 & 0 & 0 & W_u \\ -G & -I & I & -G \end{bmatrix}}_{P} \begin{bmatrix} u_{\Delta i} \\ u_{\Delta o} \\ w \\ u \end{bmatrix} \tag{11}$$

It can be observed that the obtained generalized plant is a matrix with 10 outputs and 8 inputs.

2.3 Interpretation of the uncertainty weights

The uncertainty weights are used to represent the range of frequencies in which the system behaviour is unknown. As previously stated, the diagonal terms of the weight W_i are the same, and thus only the first of them has been plotted in Figure 3. Nevertheless, its behaviour and interpretation is also valid for the weight of the second component. This also applies for Figure 4, where only W_{o1} is plotted .

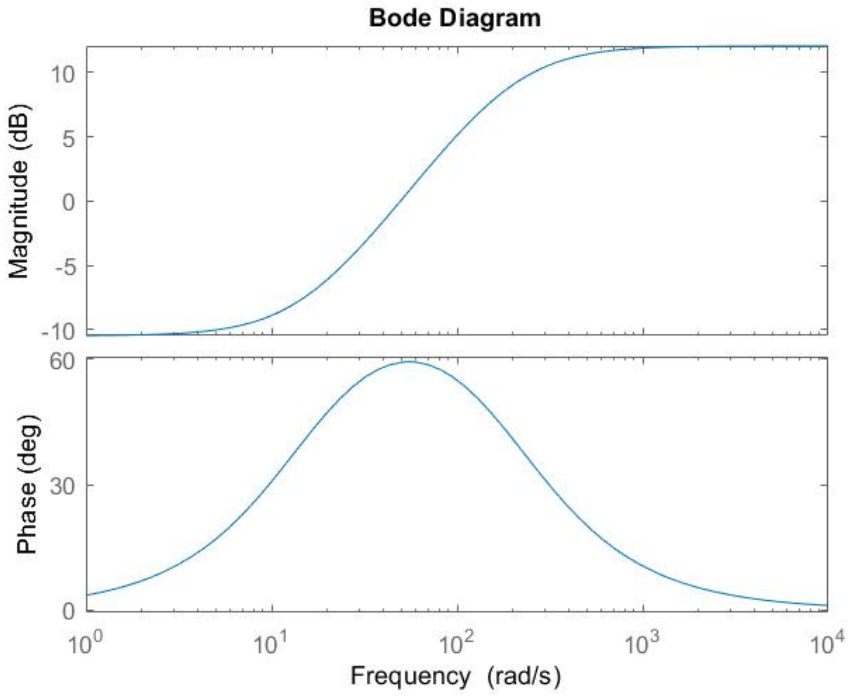

Figure 3: Bode Plot of the input uncertainty weight

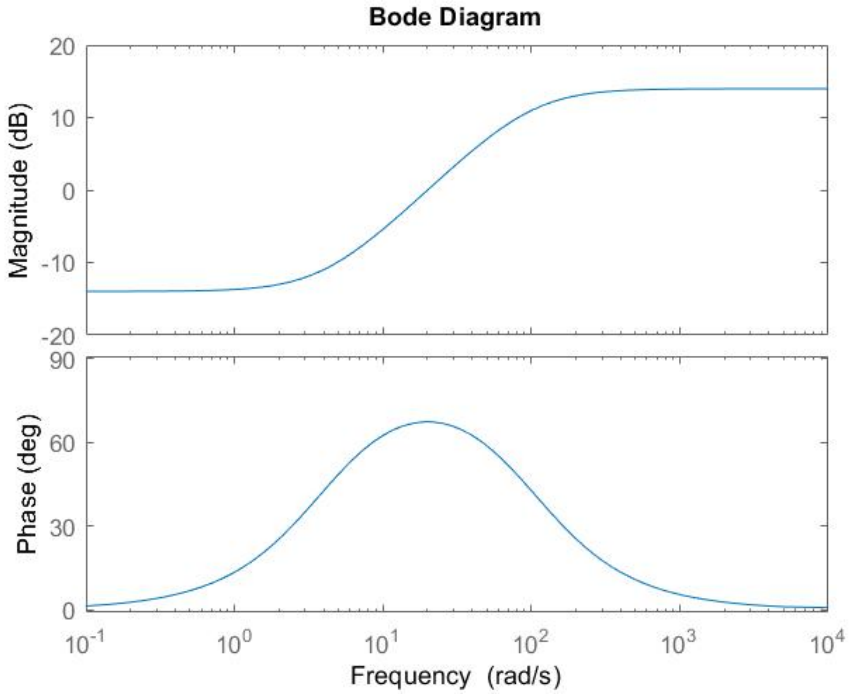

Figure 4: Bode Plot of the output uncertainty weight

One possible explanation for the weights structure and derivation is that they represent unmodelled dynamics uncertainty. Unmodelled dynamics include unknown dynamics of finite or even infinite order, and are generally represented using a multiplicative weight of the form[1]:

$$w_I(s) = \frac{\tau s + r_0}{(\tau / r_\infty)\, s + 1} \tag{12}$$

where r_0 is the relative uncertainty at steady-state, $1/\tau$ is approximately the frequency at which the relative uncertainty reaches 100%, and r_∞ is the magnitude of the weight at high frequency (typically, $r_\infty > 2$).

The weights derivation will be discussed following this possibility, and several analysis will be performed to address if this hypothesis is plausible. The expressions for W_i and W_o are hereafter reminded to facilitate the comparison with the general structure of expression 12.

$$W_{i_1} = W_{i_2} = \frac{\frac{1}{16\pi} s + 0.3}{\frac{1}{64\pi} s + 1} \tag{13}$$

$$W_{o_1} = W_{o_2} = \frac{0.05s + 0.2}{0.01s + 1} \tag{14}$$

Moreover, the mathematical expressions of the weights (Equation 13 and 14) will be also related to their Bode diagrams. The magnitude plot of the Bode diagrams of W_i and W_o are shown in Figure 5 and Figure 6, respectively. Their $y - axis$ is plotted in absolute value and they include some labels with characteristic points that will make it easier to relate them to expression 12.

The input uncertainty weight can represent the uncertainty in the actuators dynamics. Comparing expressions 12 and 13, it can be stated that the relative uncertainty of the actuators behaviour at steady-state is 30% ($r_0 = 0.3$). This information also appears in the magnitude of the Bode diagram of Figure 5. The steady-state value of the diagram of Figure 5 can be obtained by looking at the curve values for very low frequencies (leftmost label), which matches with $r_0 = 0.3$.

In addition to this, the comparison between expressions 12 and 13 shows that the relative uncertainty of W_i reaches 100% at $16\pi \approx 50$ $[rad/s]$ ($\tau = 1/16\pi$). This can be also checked by looking at the second label of Figure 5, which indicates that the magnitude of the diagram equals 1 when the frequency is 50 $[rad/s]$.

Finally, one can observe that the magnitude of the weight at high frequency should be 4, since the comparison yields $r_\infty = 4$ ($64\pi/16\pi = 4$). Once more, this matches the data in the rightmost label in Figure 5, and thus supports the hypothesis that the weights describe the influence of the system unmodelled dynamics. In essence, this interpretation explains how W_o could have been derived from the knowledge of the actuation dynamics uncertainty (30% at steady-state, 100% at 50 $[rad/s]$ and 400% for high frequencies).

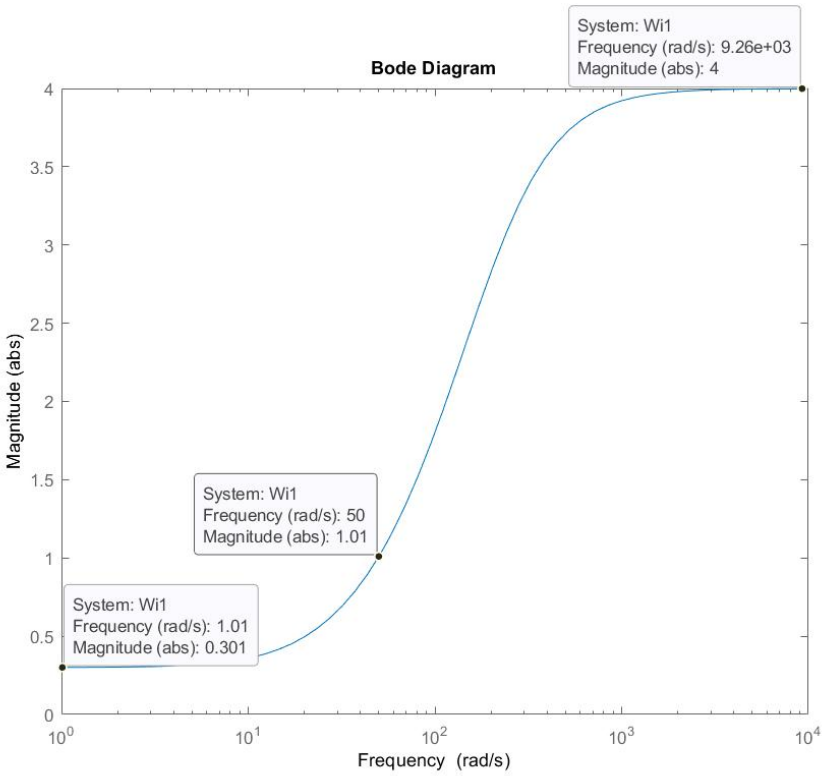

Figure 5: Magnitude plot of the Bode diagram of the input uncertainty weight in absolute value

The output uncertainty weight represents the uncertainty in the sensors behaviour. Comparing expressions 12 and 14, one can observe that the relative uncertainty of the sensors behaviour at steady-state is 20% ($r_0 = 0.2$). This matches with the steady-state value of the diagram of Figure 6, which is shown in the leftmost label and coincides with $r_0 = 0.2$.

Moreover, the comparison between expressions 12 and 13 indicates that the relative uncertainty of W_o reaches 100% at approximately 20 $[rad/s]$ ($\tau = 0.05$). The second label of Figure 6 shows that the magnitude of the Bode diagram equals 1 when the frequency is 20 $[rad/s]$, which coincides with the analysis performed based on the general structure of the expression 12.

In addition to this, it is easy to find that the magnitude of the weight at high frequency is 5 ($r_\infty = 0.05/0.01 = 5$), what coincides with the rightmost label in Figure 5. In a nutshell, W_i could have been derived taking into account the sensors behaviour uncertainty at different frequencies (20% at steady-state, 100% at 20 $[rad/s]$ and 500% at high frequencies).

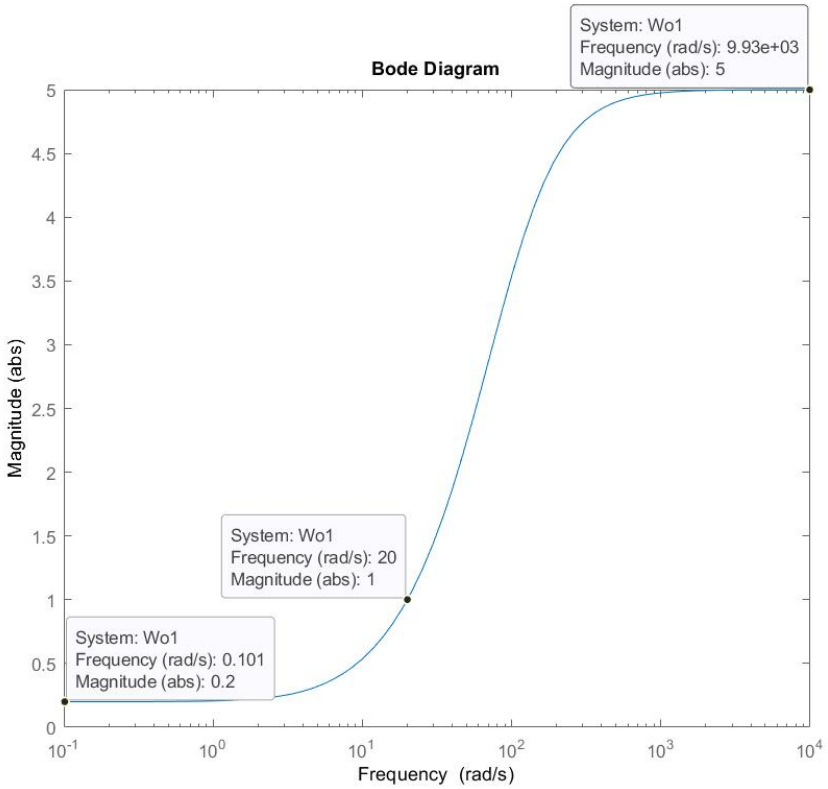

Figure 6: Magnitude plot of the Bode diagram of the output uncertainty weight in absolute value

The response of any physical system at high frequencies is difficult to model, and thus the possibility that some high-frequency dynamics of the actuators and sensors have not been included in the system is highly plausible.

Moreover, following this hypothesis, the general weight structure introduced in expression 12 suggests some uncertainty values of $20-30\%$ for the steady-state and $400-500\%$ for high frequencies. In addition to this, it indicates that the uncertainty of the actuators and sensors becomes 100% at 50 $[rad/s]$ and 20 $[rad/s]$ respectively, which is decidedly probable given the complex structure of that instruments.

All these facts strongly supports the idea that the weights represent the uncertainty introduced in the system due to the unmodelled dynamics, and that they have been derived based on the actuators and sensors uncertainty levels as previously explained.

2.4 Frequency domain analysis of the uncertain system

Based on the shape of the uncertainty weights, it is expected that the uncertain model of the plant has larger variance for high frequencies. More precisely, looking at W_o in Figure 6 suggests that the uncertainty should mainly affect the system at frequencies larger than approximately 10 $[rad/s]$, for which the uncertainty relative value exceeds 50% and should therefore be evident in the system response.

The singular values of the system relating the inputs β and τ to the outputs ω_r and z, including the uncertainty influence of W_i and W_o, have been plotted in Figure 7. Moreover, the singular values of the nominal plant have been also plotted in orange so that they can be compared to the curves with uncertainty. It can be observed that, as expected, the influence of the uncertainty is larger for frequencies after 10 $[rad/s]$.

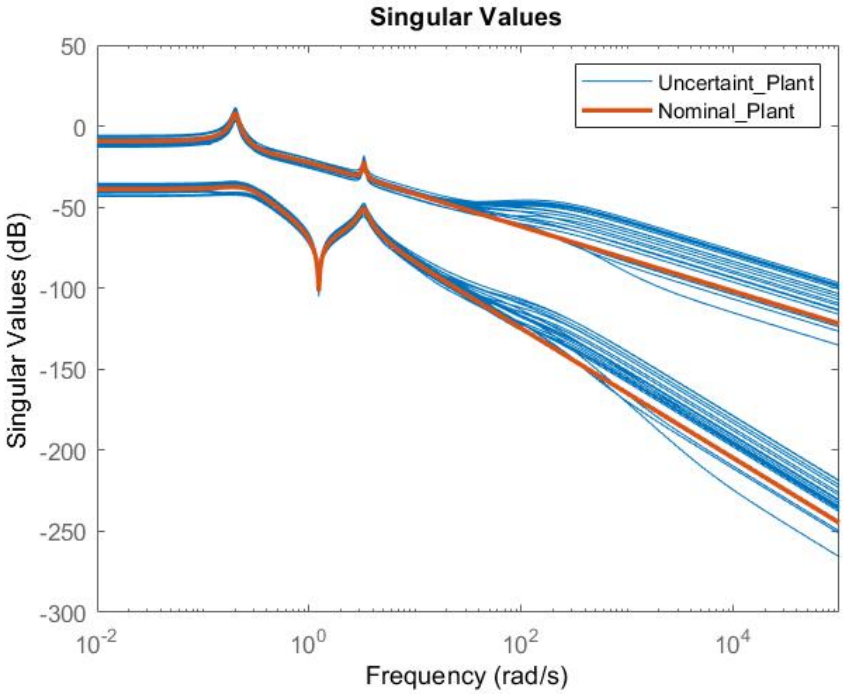

Figure 7: Singular Values of the system without disturbance

2.5 Generalized plant construction in MATLAB

Before constructing the generalized plant P, it has been calculated that the number of states it should have by taking into account the number of states that its components have. The component of P are G, which has 5 states; the performance weights W_p and W_u, which have 1 and 2 states, respectively; and the uncertainty weights W_i and W_o, which have both 2 states. Therefore, P should have 12 states, which is the addition of the states of all its components.

In addition to this, the obtained P should have 10 outputs and 8 inputs, as stated in Section 2.2. In order to obtain the Generalized plant P, the Robust Control Toolbox of Matlab has been used. After constructing P, it has been confirmed that it has 12 states, and that it is a $10x8$ matrix, and thus coincide with the mathematical description derived in Section 2.2.

2.6 Nominal and robust analysis

2.6.1 Nominal stability (NS) check

In this section, it has been checked if the system has Nominal Stability using the mixed-sensitivity controller found in Part 2 and the generalized plant P found in the previous section. As a key aspect, it shall be highlighted that in order to check for NS, one should use the nominal plant (not the whole P), and therefore the uncertainty matrices W_i and W_o do not influence the result.

For that reason, the discussion about the system NS can be performed in the same way as in Part 2, just looking at the state-space system that relates the inputs τ and β to the outputs ω_r and z, in addition to the controller of Part 2 (K).

The Generalized Nyquist theorem [1] states that a closed-loop system is stable if and only if the Nyquist Plot of $det(I + L(s))$ makes P anti-clockwise encirclements of the origin and does not cross the origin, where P is the number of unstable poles of the open-loop transfer function L(s).

The unstable poles of the open-loop transfer function $L(s)$ can be obtained by computing the poles of $G(s)K(s)$, which are the following:

$$p_1 = -34.0428 \tag{15}$$
$$p_2 = 0.0083 + 3.4260i \tag{16}$$
$$p_3 = 0.0083 - 3.4260i \tag{17}$$
$$p_4 = -0.0671 + 0.2130i \tag{18}$$
$$p_5 = -0.0671 - 0.2130i \tag{19}$$
$$p_6 = -0.0572 + 0.0637i \tag{20}$$
$$p_7 = -0.0572 - 0.0637i \tag{21}$$
$$p_8 = -0.0003 \tag{22}$$

where $p2$ and $p3$ are the RHP poles of $L(s)$.

The Generalized Nyquist Plot is shown in 8, and it can be observed that it encircles the origin two times in anti-clockwise direction (and it does not cross the origin). Therefore, it can be claimed that the closed-loop system is stable and therefore that the system has Nominal Stability.

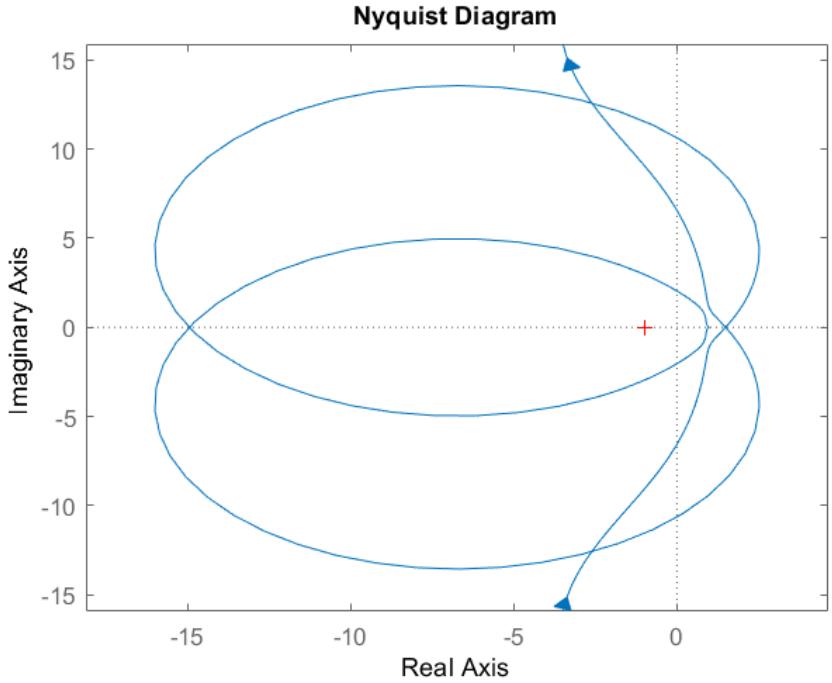

Figure 8: Nyquist diagram of $det(I + L(s))$

2.6.2 Nominal performance (NP) check

In order to address Nominal Performance, the generalized plant P and the controller K shall be used to generate the matrix N, which can be constructed using the Linear Fractional Transformation (LFT) of P and K.

N has 8 outputs and 6 inputs, since the inputs and outputs of the controller that appeared in P have been merged into N. Therefore, N can be divided in four submatrices $N_{11}, N_{12}, N_{21}, N_{22}$, that relate the uncertainty outputs vector y_Δ and the performance outputs vector z to the uncertainty inputs u_Δ and the reference input ω:

$$\begin{bmatrix} y_\Delta \\ z \end{bmatrix} = \begin{bmatrix} N_{11} & N_{12} \\ N_{21} & N_{22} \end{bmatrix} \begin{bmatrix} u_\Delta \\ w \end{bmatrix} \tag{23}$$

where

$$y_\Delta = \begin{bmatrix} y_{\Delta i} \\ y_{\Delta o} \end{bmatrix} \tag{24}$$

$$z = \begin{bmatrix} z_1 \\ z_2 \end{bmatrix} \tag{25}$$

$$u_\Delta = \begin{bmatrix} u_{\Delta i} \\ u_{\Delta o} \end{bmatrix} \tag{26}$$

In addition to this, the Structure Singular Values (SSV) of N_{22} can be used to address the NP if the LFT of N and Δ_P is performed, as shown in Figure 9. Δ_P is a full uncertainty matrix (without structure), which has 4 inputs and 2 outputs.

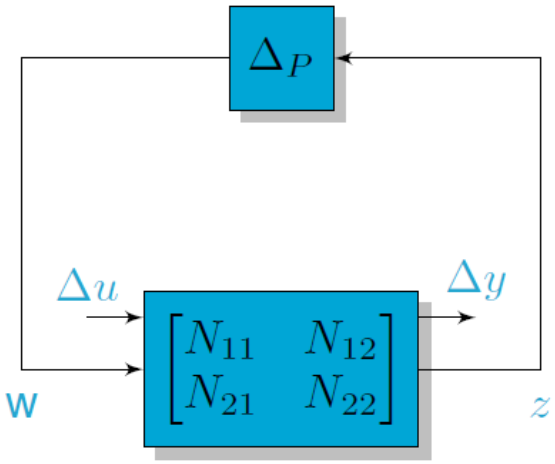

Figure 9: LFT of Δ_P and N [2]

In order to check for NP, the system shall have Nominal Stability (which has been proved to have) and also:

$$\mu_{\Delta_P}(N_{22}) < 1 \quad \forall\omega \tag{27}$$

For implementation reasons a set of ω frequencies should be specified where the μ value evaluation is executed. By looking at the singular value plot of the system it can be seen that the relevant dynamics are in the range of $10^{-3} - 10^{3}[rad/sec]$. The ω vector was defined to consists of 1000 points equally distributed in this range on a logarithmic scale. The plot of the SSV of N_{22} is shown in Figure 10, which shows that they lie below 1 for all the frequencies.

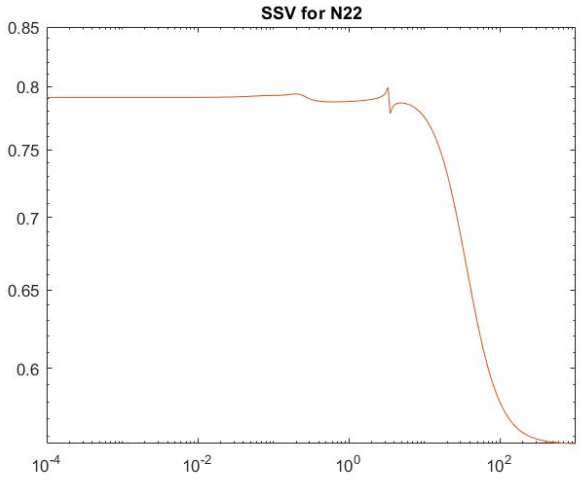

Figure 10: Structured Singular Values of N_{22}

The μ value of N_{22} has been calculated using Matlab, obtaining a value of 0.7993, which coincides with Figure 10. Since this value is smaller than 1, the system has Nominal Performance.

2.6.3 Robust stability (RS) check

The system Robust Stability can be checked by performing the Linear Fractional Transformation between the uncertainty matrix Δ (defined in expression 1) and N, to obtain the system shown in Figure 11:

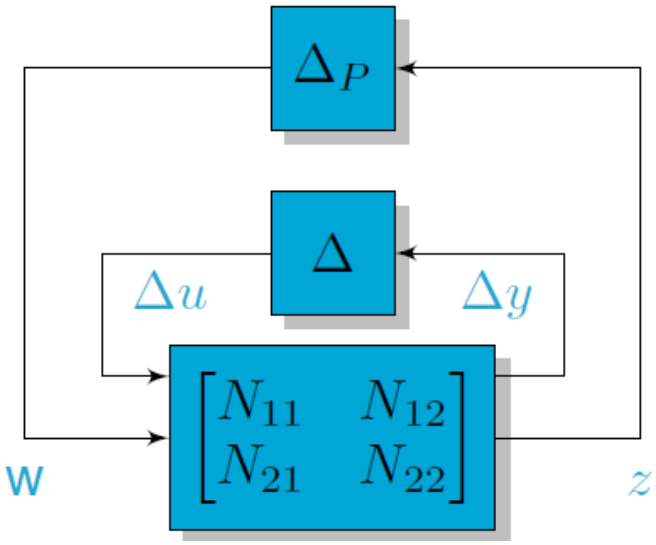

Figure 11: LFT of Δ and N [2]

At this point, the system can be claimed to have Robust Stability if it has Nominal Stability (already proven), and if:

$$\mu_{\Delta}(N_{11}) < 1 \quad \forall\omega \tag{28}$$

The plot of the SSV for N_{11} is shown in Figure 12, in which it can be observed that all the values are below 1 (the same ω vector was used as for NP).

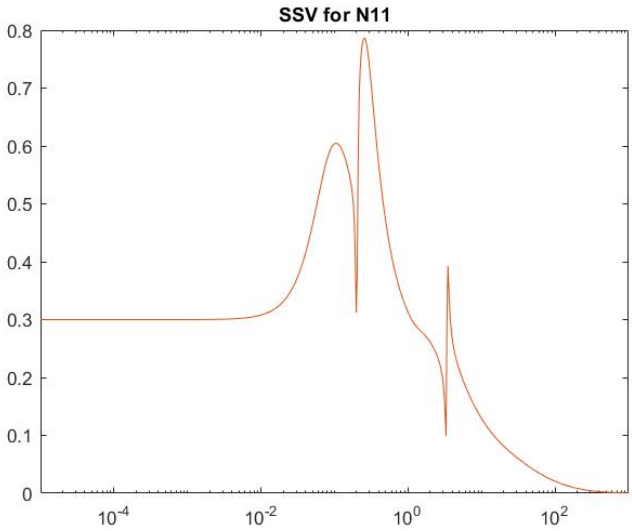

Figure 12: Structured Singular Values of N_{11}

A μ value of 0.7865 was obtained using the Robust Control Toolbox of Matlab, which means that the system has Robust Stability.

2.6.4 Robust performance (RP) check

In order to check the system Robust Performance, the two uncertainty matrices previously used (Δ, Δ_P) can be used to perform the LFT with N, as shown in Figure 13.

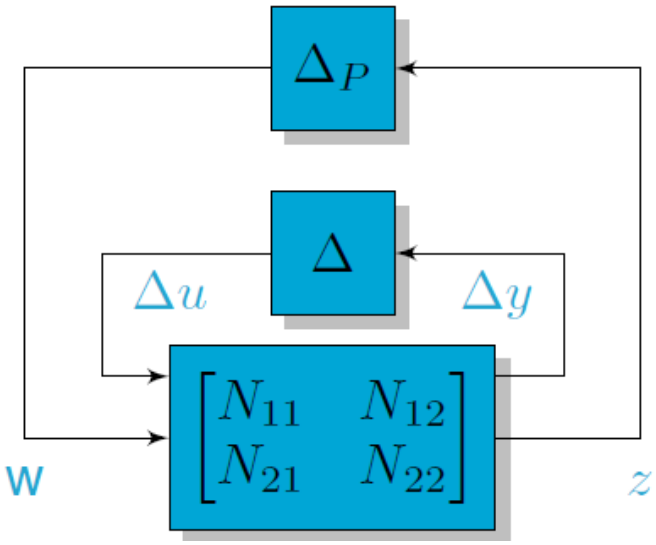

Figure 13: LFT of the uncertainty matrices and N

The Structured Singular Values of N can be therefore used to address the system Robust Performance, as follows:

$$\mu_{\hat{\Delta}}(N) < 1 \quad \forall\omega \tag{29}$$

where

$$\hat{\Delta} = \begin{bmatrix} \Delta & 0 \\ 0 & \Delta_P \end{bmatrix} \tag{30}$$

The Structured Singular Values of N have been plotted in Figure 14, which shows that some of the values are larger than 1 (the same ω vector was used as for NP).

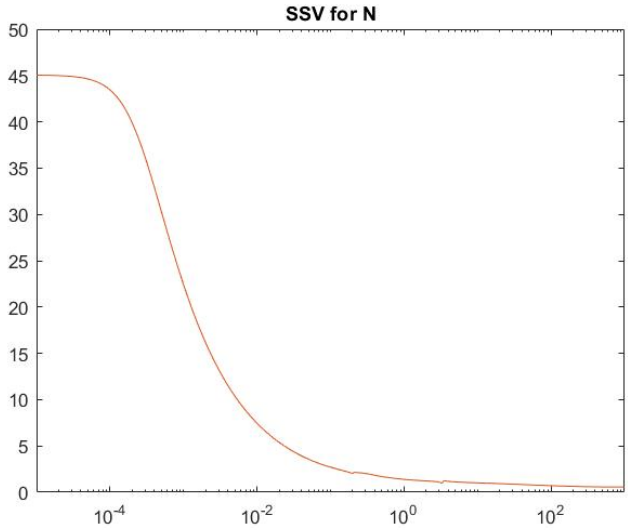

Figure 14: Structured Singular Values of N

Since the equation 29 is not satisfied, it can be stated that the system does not have RP. This has been also confirmed by calculating the μ value for N, which reaches 45.0379.

2.7 Relationships in case of NP check

The structure of Δ_P is a key fact to address the relationship between the value of μ and the H_∞ norm in the mixed-sensitivity problem. The H_∞ norm provides the largest singular value of the transfer function that relates the reference inputs ω to the performance outputs z, which coincides with the block N_{22} in the Nominal Performance check (Equation 23).

In contrast, μ is obtained from the LFT of Δ_P and N_{22}. However, since the Δ_P matrix is full (unstructured), the structured singular values of $N_{22}\Delta_P$ coincide with the singular values of N_{22}, and thus with the H_∞ norm value of the mixed-sensitivity problem.

This has been confirmed using Matlab, which provides an H_∞ norm value of N_{22} of 0.7993, which coincides with the value of μ obtained for the NP analysis.

3 Robust controller synthesis

Robust performance can be achieved by using controller synthesis algorithm that considers also this requirement, for example the μ synthesis. The algorithm uses the D-K iteration that is described in more details in the following sections.

3.1 Structure of the D scaling matrix

Figure 15 shows the structure how the D scaling is applied. M describes the connection of the closed loop system with the Δ block. Using the same notation as in the lectures it would be N_{11}[2]. It can be shown that this scaling will not affect a diagonal Δ matrix but it can scale the singular values of the M matrix[1].

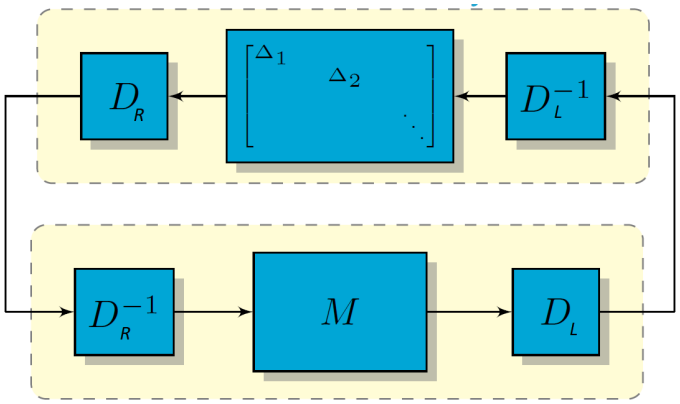

Figure 15: The D scaling applied[2]

A D scaling matrix is updated in each iteration of the method. Despite its values are previously unknown its structure can be described analytically based on how the uncertainty in the system is modelled.

The Δ uncertainty block derived for the robust performance analysis is used here. There is a connection between the structure of Δ and the structure of D. Where full uncertainty block is used in Δ, the corresponding element in D is an identity block. Also diagonal structure in Δ results in diagonal positioning in D. This scaling is applied to the N closed loop system. Since N is not square 2 separate (but similar) scaling matrices are created: D_L for the multiplication from left and D_R for the multiplication from the right (its inverse is used):

$$\Delta_i = \begin{bmatrix} \Delta_{i1} & 0 \\ 0 & \Delta_{i2} \end{bmatrix} \quad \longrightarrow \quad D_L = \begin{bmatrix} d_{i1} & 0 \\ 0 & d_{i2} \end{bmatrix} \quad D_R = \begin{bmatrix} d_{i1} & 0 \\ 0 & d_{i2} \end{bmatrix} \tag{31}$$

$$\Delta_o = \begin{bmatrix} \Delta_{o1} & 0 \\ 0 & \Delta_{o2} \end{bmatrix} \quad \longrightarrow \quad D_L = \begin{bmatrix} d_{o1} & 0 \\ 0 & d_{o2} \end{bmatrix} \quad D_R = \begin{bmatrix} d_{o1} & 0 \\ 0 & d_{o2} \end{bmatrix} \tag{32}$$

$$\Delta_p = \begin{bmatrix} \Delta_{p11} & \Delta_{p12} \\ \Delta_{p21} & \Delta_{p22} \\ \Delta_{p31} & \Delta_{p32} \\ \Delta_{p41} & \Delta_{p42} \end{bmatrix} \quad \longrightarrow \quad D_L = \begin{bmatrix} 1 & 0 & 0 & 0 \\ 0 & 1 & 0 & 0 \\ 0 & 0 & 1 & 0 \\ 0 & 0 & 0 & 1 \end{bmatrix} \quad D_R = \begin{bmatrix} 1 & 0 \\ 0 & 1 \end{bmatrix} \tag{33}$$

$$\Delta = \begin{bmatrix} \Delta_i & 0 & 0 \\ 0 & \Delta_o & 0 \\ 0 & 0 & \Delta_p \end{bmatrix} \quad \longrightarrow \quad D_L = diag(d_{i1}, d_{i2}, d_{o1}, d_{o2}, I_{4x4}) \quad D_R = diag(d_{i1}, d_{i2}, d_{o1}, d_{o2}, I_{2x2}) \tag{34}$$

In the D-K iteration the K step consists of an optimization with a controller included. In the implementation it is practical to define extended D'_L and D'_R matrices. These can be used to scale the generalized plant rather than the closed loop system (N). Since the control input u and the controller input v should not be scaled the matrices are extended with identity blocks.

$$D'_L = diag(d_{i1}, d_{i2}, d_{o1}, d_{o2}, I_{6x6}) \quad D'_R = diag(d_{i1}, d_{i2}, d_{o1}, d_{o2}, I_{4x4}) \tag{35}$$

3.2 D-K iteration manually and using dksyn

3.2.1 Description of the method

Each iteration in the this method consists of 2 steps, 2 separate optimization. First the D matrix is optimized given a certain controller (Equation 36), then the controller is optimized given a certain D scaling (Equation 37). The iterations stops when there is no further improvement in the objective value, which is the peak value (or infinity norm) of the μ structured singular value. To achieve robust performance this value should converge bellow (or at least a close to) 1.

$$\min_{D_L(j\omega), D_R(j\omega)} \bar{\sigma}(D_L(j\omega) N(j\omega) D_R^{-1}(j\omega)) \tag{36}$$

$$\min_K \|D_L N(K) D_R^{-1}\|_\infty \quad \longrightarrow \quad \min_K \|lft(D'_L P D_R^{'-1}, K)\|_\infty \tag{37}$$

The optimization of the D scaling matrices are done using a certain set of preliminary ω frequencies (1000 points ranging from 10^{-3} to 10^3 [rad/s]). At each frequency an optimal $D_L(j\omega)$ and $D_R(j\omega)$ is determined (mussv and mussvextract functions in MATLAB). When these optimal points are determined a transfer function can be fitted on these curves individually, thus building a D_L and a D_R transfer matrix. In the assignment 6th order transfer was used for the fitting.

The K optimization step is an H_∞ controller synthesis on the scaled plant using the extended scaling matrices (Equation 37).

The *dksyn* function (Robust Control Toolbox) executes similar steps and also its result is similar.

3.2.2 Results

Figure 16 shows the peak μ value evolution of the closed loop system during the manual and the automated (dksyn) D-K iterations. The results are generally similar, the peak μ value in case of the manual tuning is 1.15 and in case of the dksyn it is 1.14. These values are not bellow 1, which would be the strict condition for robust performance. But since these are quite close to it, it can be stated that robust performance is achieved.

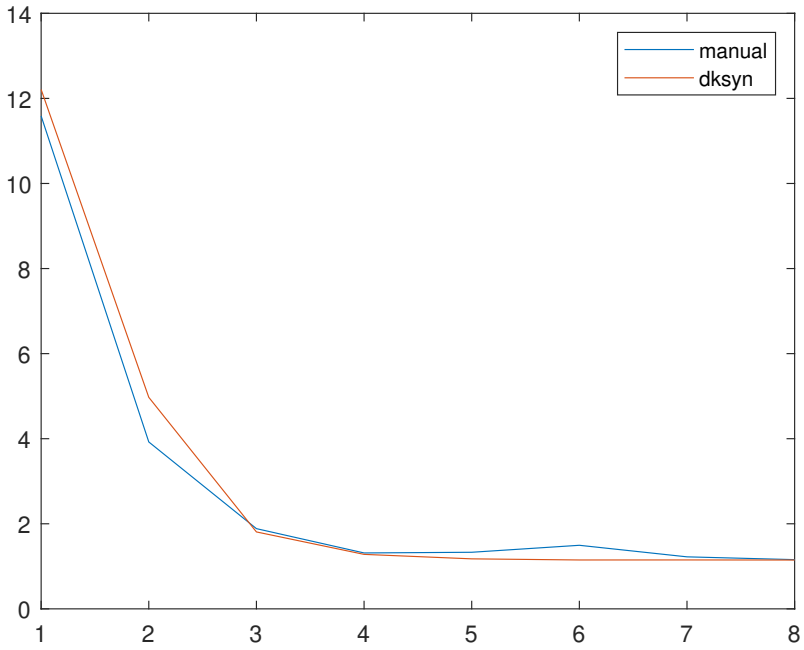

Figure 16: μ value evolution during 8 D-K iteration

There are also some differences in the controller order. In case of the manual tuning the order is 58 and using dksyn it is 48 (after using the minreal MATLAB command).

3.3 Time-domain simulations, frequency domain comparisons

Time-domain simulations can show some differences between the closed loop systems with the robust controller and with the nominal one. Figure 17 shows the reference tracking step response of the nominal plant. It is expected that with the robust controller the system will have higher overshoot and/or higher settling time. The overshoot is indeed a bit higher, but the settling times are approximately the same.

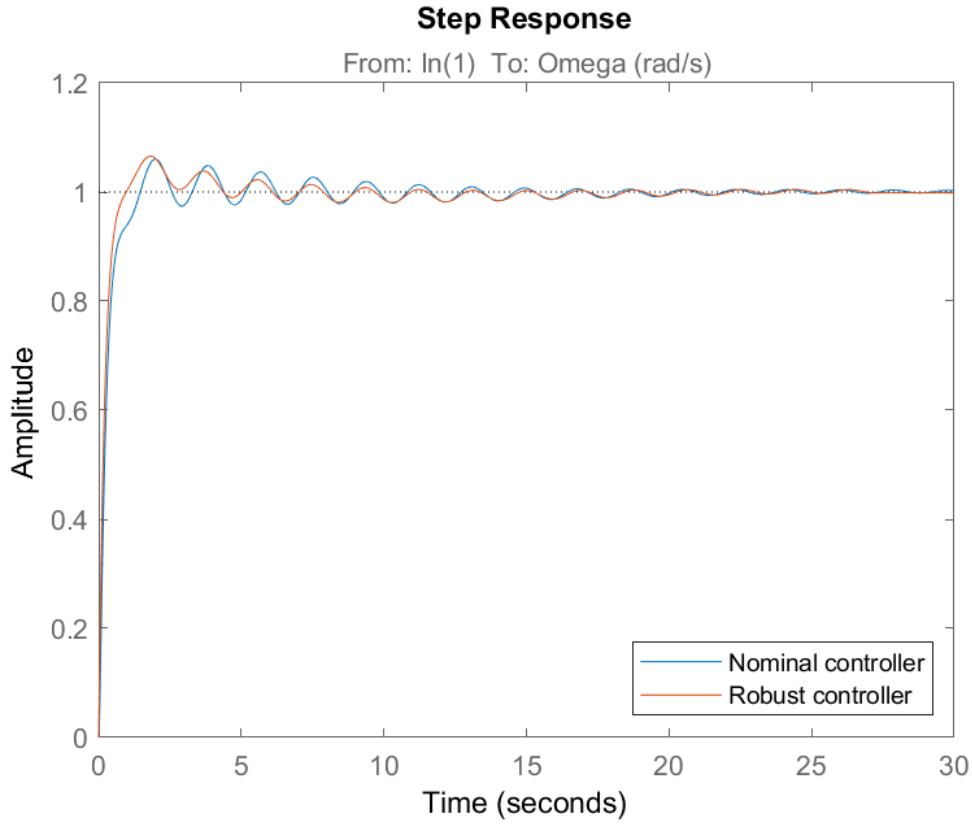

Figure 17: Controller comparison for the nominal plant (reference tracking)

Since in MATLAB the uncertain plant can also be simulated with a number of different realizations the step responses can also be compared in case of uncertainty. Figure 18 shows that both controller achieves robust stability. It was expected since it was previously shown for the nominal controller and the robust controller is designed this way. It can also be seen that the robust controller has a more consistent response (the variation in the different realizations is smaller) which is an indication of the robust performance. The disturbance rejection check (Figure 19) also shows that the response with robust controller is more consistent.

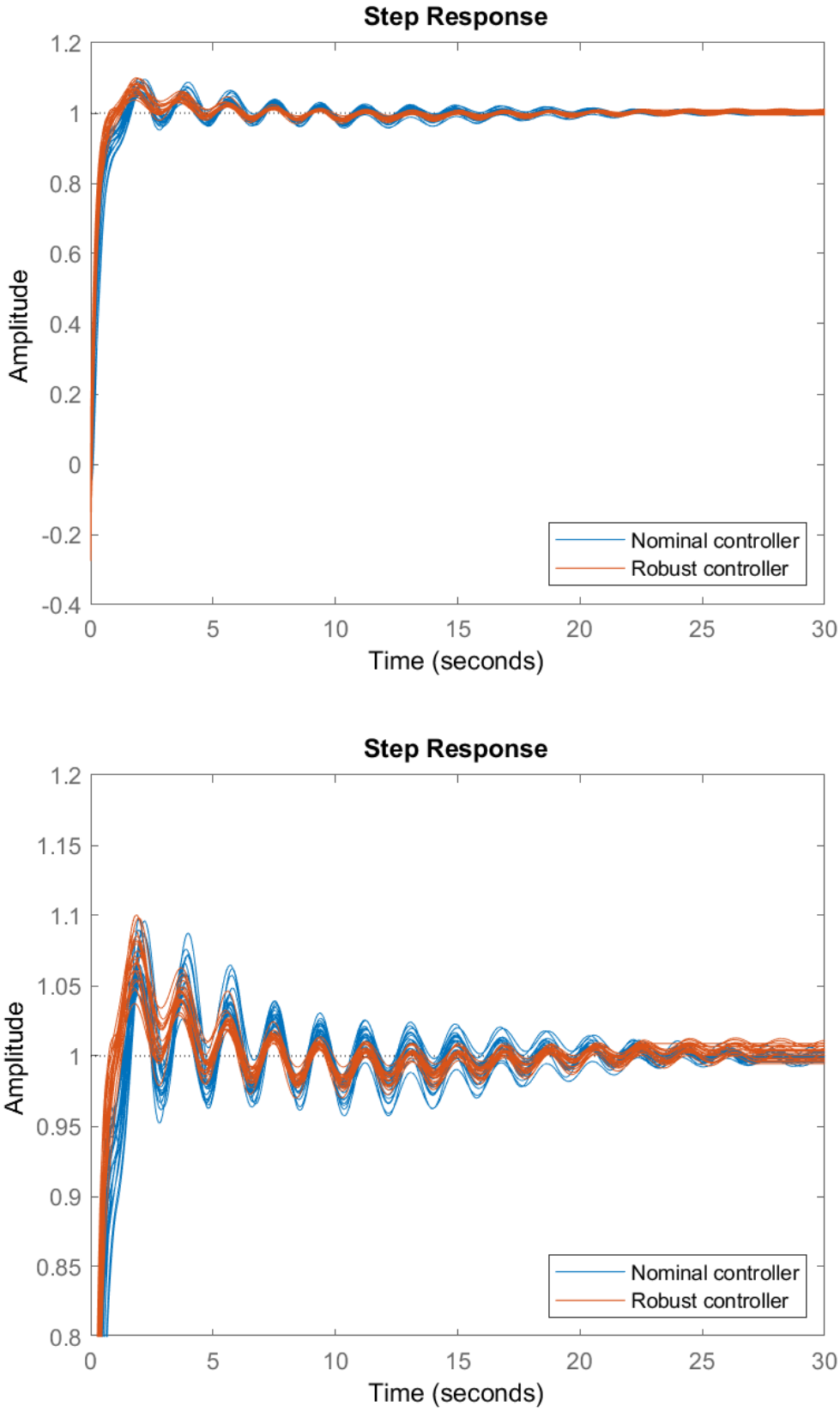

Figure 18: Controller comparison for the uncertain plant (reference tracking)

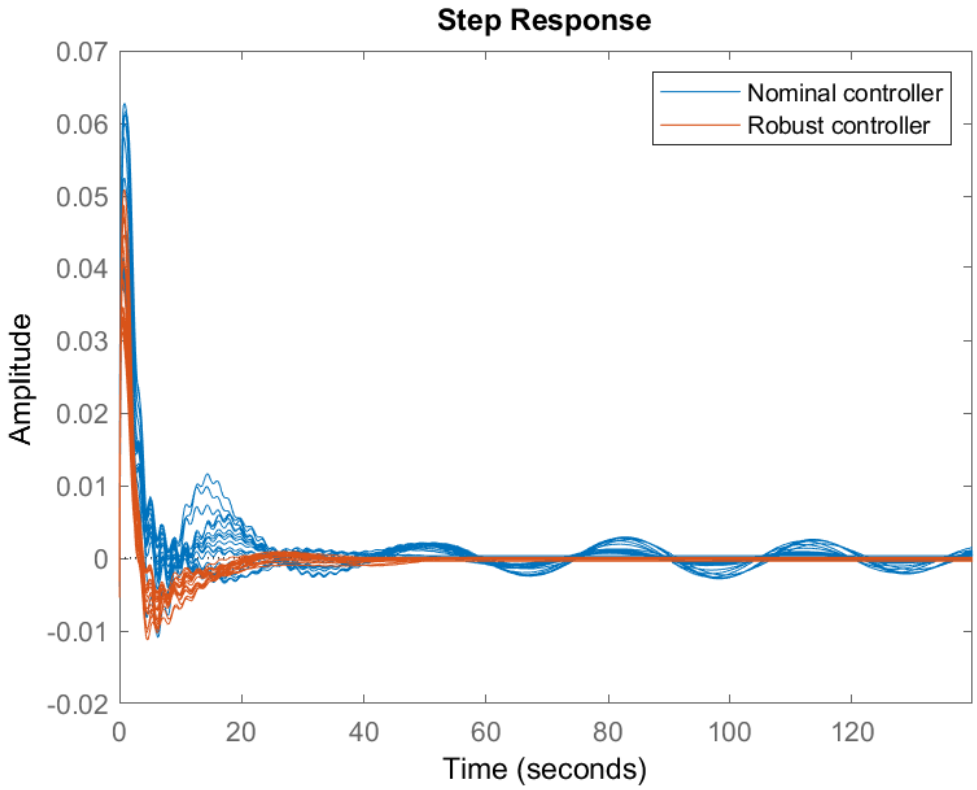

Figure 19: Controller comparison for the uncertain plant (disturbance rejection)

Frequency-domain comparisons can also be made using the sensitivity and complementary sensitivity functions. For simplicity only the complementary sensitivity function is used here (Figure 20). It can be seen from the minimum and maximum singular value plot of this function that although the plots are similar for the robust and the nominal controller a main difference is a removed peak around $0.2[rad/s]$. The peak in the complementary sensitivity function means that there is also a peak in the sensitivity plot. It is also somewhat intuitive that by removing this peak the effect of the uncertainty will be less significant.

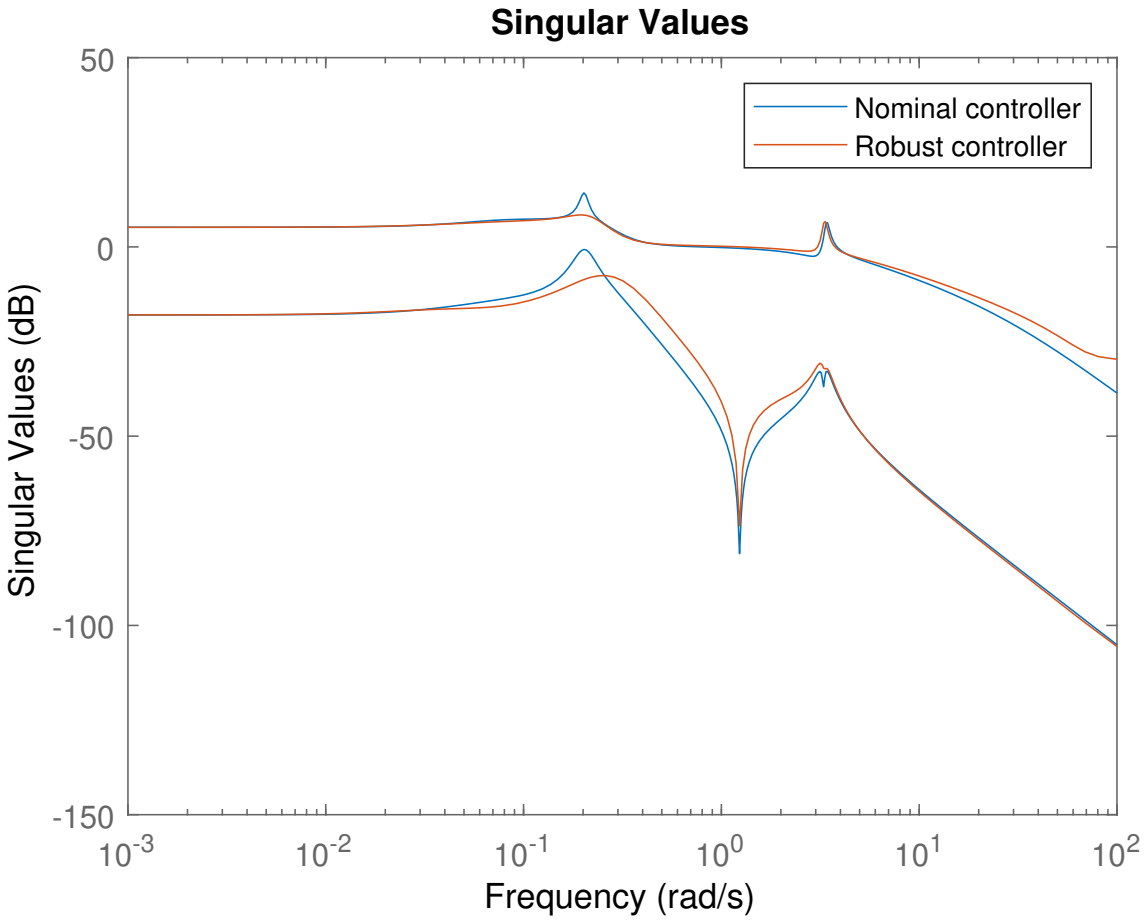

Figure 20: Complementary sensitivity singular value plot of the closed loop systems

4 Summary

In Part 1 of the assignment PID-type controller was designed to satisfy either reference tracking or disturbance rejection requirements using only the β pivot position input and considering only the generator speed output. It was shown that the RHP zeros in the system pose some limitations on the achievable bandwidth.

In Part 2 both the β angle and the τ generator torque inputs were used for the control and the ω generator speed and the z tower displacement were measured. There controllers were synthesised using H_∞ design. It was shown that the MIMO system does not have RHP zeros and indeed much better performance could have been achieved using multivariable control. In Part 2.1 it was shown that the operating frequencies of the 2 controller outputs can be shaped via the input weights in the mixed-sensitivity design.

In this Part 3 first the robustness properties of the controller from Part 2 were analysed (stability and performance). It was shown that if robust performance requirements should be satisfied then μ controller synthesis can be used. The designed robust controller was shown to have more consistent time-domain responses under uncertainty than the nominal controller.

References

[1] Sigurd Skogestad and I Postlethwaite. "Multivariable Feedback Control: Analysis and Design". In: vol. 2. Jan. 2005.

[2] Jan-Willem van Wingerden. *Lecture slides in Robust Control*. 2020-2021.